

Hydrogen Bonding Patterns and DFT Studies of (4-Acetylphenyl)amino 2,2-Dimethylpropanoate and (E)-1-(4-Aminophenyl)-3-[4-(dimethylamino)phenyl]prop-2-en-1-one

Rama Kant · Biswajit Maiti · Satish Kumar Awasthi · Alka Agarwal

Received: 14 March 2014 / Accepted: 3 July 2014 / Published online: 16 July 2014
© Springer Science+Business Media New York 2014

Abstract The (4-acetylphenyl)amino 2,2-dimethylpropanoate (**1**) and (E)-1-(4-aminophenyl)-3-[4-(dimethylamino)phenyl]prop-2-en-1-one (**2**), were synthesized and characterized by elemental analysis, FT-IR, ¹H NMR, ¹³C NMR and single crystal X-ray diffraction techniques. Both compounds **1** and **2** crystallized in orthorhombic crystal system with Pbc_a and P212121 space group respectively, having the unit cell parameters: $a = 11.7220(12) \text{ \AA}$, $b = 14.4580(13) \text{ \AA}$, $c = 15.7853(12) \text{ \AA}$, $\beta = 90^\circ$, Volume = $2675.2(4) \text{ \AA}^3$, $Z = 8$ for **1** and $a = 6.1146(5) \text{ \AA}$, $b = 9.0567(8) \text{ \AA}$, $c = 26.079(3) \text{ \AA}$, $\beta = 90^\circ$, Volume = $1444.2(2) \text{ \AA}^3$, $Z = 4$ for compound **2**. The crystal structures of both compounds (**1** and **2**) are stabilized by N–H...O strong intermolecular hydrogen bonding forming C₁(**8**) motifs. In compound **1**, the molecules are linked by three C–H...O intramolecular H-bond forming S(**6**) motifs. In compound **2**, the molecules are linked by C–H...N intermolecular H-bond exhibiting C₁(**12**) motif and C–H...O intramolecular H-bond leading to S(**5**) motif. Crystallographic and vibrational data are compared with the results of density functional theory (DFT) method at the B3LYP/6-31G(d,p) level. The electronic (UV–vis) spectra was calculated by using the TD-DFT method and correlated with experimental spectra.

Keywords Hydrogen bonding · DFT · Graph-set motifs · (4-Acetylphenyl)amino 2,2-dimethylpropanoate · (E)-1-(4-aminophenyl)-3-[4-(dimethylamino)phenyl]prop-2-en-1-one

Introduction

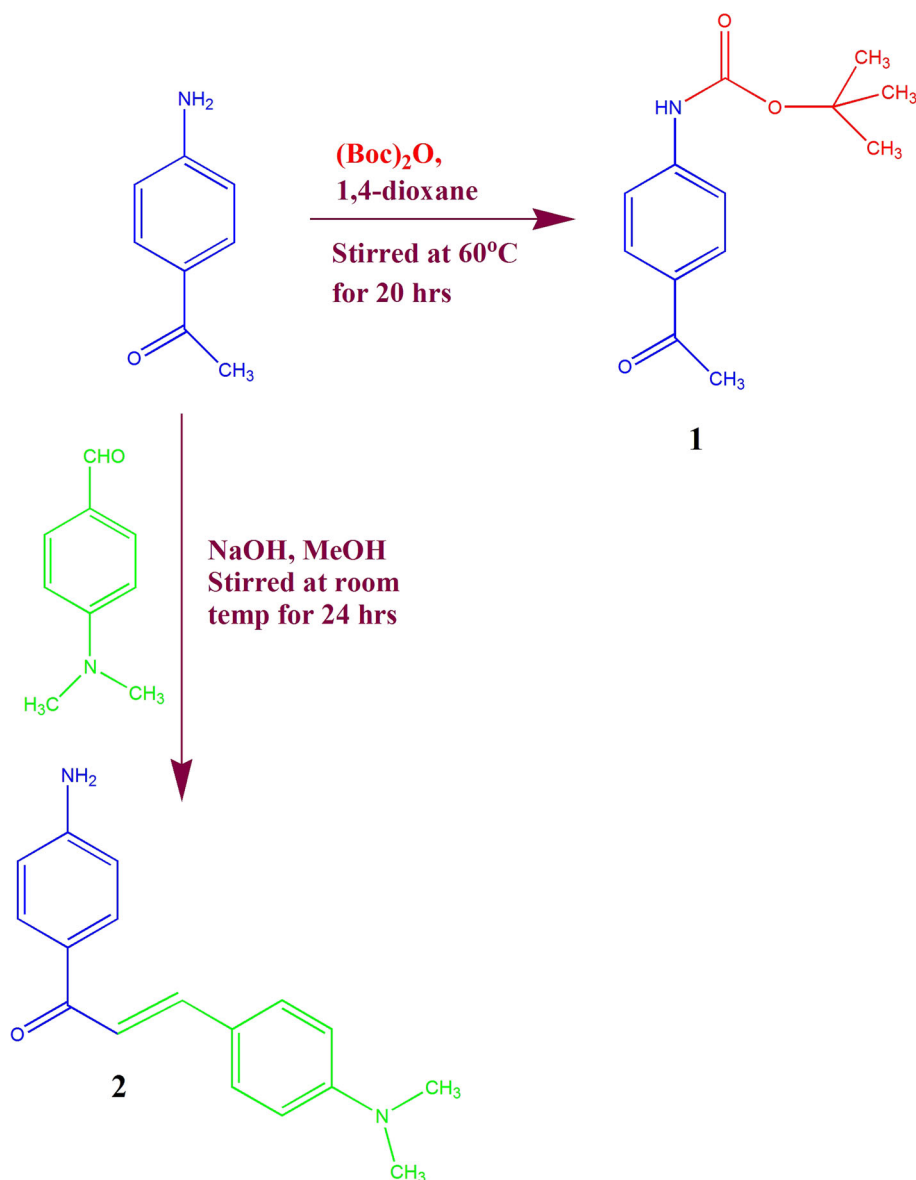
Chalcones are Michael acceptors, bearing the 1,3-diaryl-prop-2-en-1-one framework which are usually prepared by Claisen–Schmidt condensation method between aromatic aldehydes and ketones under homogeneous conditions. They contain two aromatic rings which are joined through α , β unsaturated ketone, and this unique structure is responsible for various activities of these molecules [1]. Chalcones are naturally occurring compounds which belong to the flavonoid family [1, 2], and used for drug design and development. During the past decade, synthetic modifications in chalcones skeleton enhance their bioactivities. The chalcones and their derivatives have excellent anticancer [3, 4], antimalarial [5], anti-inflammatory [6], antileishmanial [6], antituberculosis [7], nitric oxide inhibition [8], antimutagenic [9], analgesic, antipyretic, antioxidant [10, 11], antibacterial, anti-HIV [12], antifungal [13], antiprotozoal activities [14], and are also reported to be gastric protectant [15], antimutagenic, and antitumorogenic [16]. The commercially available 4-aminoacetophenone is used in synthesis of flavaniline [17], antibacterial [18], anti-inflammatory [19], anti HIV [20] agents and an oral hypoglycemic drug such as acetohexamide [21]. In the view of the above mentioned facts, we designed and synthesized (4-acetylphenyl)amino-2,2-dimethylpropanoate (**1**) and (E)-1-(4-aminophenyl)-3-[4-(dimethylamino)phenyl]prop-2-en-1-one (**2**) (Scheme 1). Our research group mainly works on antimicrobial compounds [22, 23]. Recently we have reported several X-rays analysis of small molecules [24–30]. In this study, we are reporting for the first

R. Kant · A. Agarwal (✉)
Department of Medicinal Chemistry, Institute of Medical Sciences, Banaras Hindu University, Varanasi 225001, UP, India
e-mail: alka_ag_2000@yahoo.com

B. Maiti
Department of Chemistry, Faculty of Science, Banaras Hindu University, Varanasi 225001, UP, India

S. K. Awasthi
Chemical Biology Research Laboratory, Department of Chemistry, University of Delhi, Delhi 110007, India

Scheme 1 Schematic representation of synthesis of (4-acetylphenyl)amino 2,2-dimethylpropanoate (**1**) and (E)-1-(4-aminophenyl)-3-[4-(dimethylamino)phenyl]prop-2-en-1-one (**2**)



time the crystal structure, hydrogen bonding patterns and DFT calculations for protected compound “(4-acetylphenyl)amino 2,2-dimethylpropanoate” (**1**) and a chalcone “(E)-1-(4-aminophenyl)-3-[4-(dimethylamino)phenyl]prop-2-en-1-one” (**2**). It is found that the computed DFT results corroborate experimental predictions for both the compounds (**1** and **2**).

Experimental

Reagents and Techniques

AR grade di-*tert*-butyldicarbonate, 4-aminoacetophenone, 1,4-dioxane, 4-dimethylaminobenzaldehyde were purchased from Aldrich. Other reagents and solvents were used without further purification. Melting points were

determined by open capillary method taken with a Sciencetech melting point apparatus. Elemental (C, H, O and N) analysis were made on a Perkin–Elmer Model 240B automatic analyser. IR spectra were recorded on a Perkin Elmer Spectrum Version 10.03.05 FT-IR spectrometer in the range of $400\text{--}4000\text{ cm}^{-1}$ employing a KBr disc. UV–vis spectra was measured on a analytikjana model SPECORD 250 spectrophotometer using methanol solutions in the $220\text{--}560\text{ nm}$ range and Fluorescence spectra was recorded VARIAN CARY ECLIPSE. Nuclear magnetic resonance (^1H and ^{13}C) spectra were recorded on JEOL AL 300 FTNMR (300 MHz for ^1H and 75 MHz for ^{13}C) spectrometer with tetramethylsilane (TMS) as the internal reference and chemical shifts are measured in δ ppm downfield from tetramethylsilane. Standard 5 mm probe was used for the ^1H and ^{13}C NMR measurements. X-ray

diffraction was carried out on an Oxford Diffraction Xcalibur four-circle diffractometer with Eos CCD-detector.

Synthesis and Characterization of (4-acetylphenyl)amino 2,2-dimethylpropanoate (**1**)

The compound **1** was synthesized by reported procedure [31]. Di-*tert*-butyldicarbonate (3.23 ml, 14.06 mmol) was added to the stirred solution of 4-aminoacetophenone (2 g, 14.81 mmol) in 1,4-dioxane (36.5 ml). The reaction mixture was stirred at 60 °C for 20 h. After completion of reaction as monitored by TLC, the solvent was removed and the residue was dissolved in ethyl acetate, washed with brine solution (2 × 50 ml) and water (2 × 50 ml), dried over Na₂SO₄ and concentrated in vacuo. The resulting solid was recrystallized from methanol. Transparent light yellow crystals were obtained from methanol by slow evaporation at room temperature after few days. Yield 2.2 g (67.50 %), m.p. 134–135 °C, R_f = 0.66 (98:2, dichloromethane : methanol), Mass m/z 235 (M⁺). ¹H NMR (CDCl₃, 300 MHz, ppm) δ: 1.53 (s, 9H, 3CH₃), 2.56 (s, 3H, COCH₃), 6.76 (s, 1H, NH), 7.44 (d, *J* = 8.4 Hz, 2H, ArH), 7.89 (d, *J* = 8.7 Hz, 2H, ArH). ¹³C NMR (CDCl₃, 75 MHz, ppm) δ: 26.32 (C of CH₃ in methyl keto group), 28.20 (C of CH₃ in *t*-butyl group), 81.17 (C of C–O in *t*-butoxy group), 117.35, 129.78, 131.66, 142.99 (C of Aromatic ring), 152.19 (C of O–C=O), 196.99 (C=O). Elemental analysis (Perkin–Elmer 240B elemental analyzer) Calculated for: C₁₃H₁₇NO₃ (%) Calculated C = 66.38, H = 7.23, N = 5.96, O = 20.43; Found C = 66.32, H = 7.43, N = 5.66, O = 20.53.

Synthesis and Characterization of (E)-1-(4-aminophenyl)-3-[4-(dimethylamino)phenyl]prop-2-en-1-one (**2**)

The compound **2** was synthesized by reported method [32]. Briefly, NaOH (0.178 g, 4.45 mmol) was added to the well stirred solution of 4-aminoacetophenone (0.200 g, 1.48 mmol) and the 4-dimethylaminobenzaldehyde (0.221 g, 1.48 mmol) in methanol (3 ml). The reaction mixture was further stirred for 24 h at room temperature. The completeness of reaction was monitored by TLC, ice cold water was added and neutralized with 1 N HCl. Transparent yellow crystals were obtained from methanol by slow evaporation at room temperature after few days. Yield 0.340 g (86.27 %), m.p. 149–150 °C, R_f = 0.70, (98:2, dichloromethane : methanol), Mass m/z 266 (M⁺). ¹H NMR (CDCl₃, 300 MHz, ppm) δ: 3.03 (s, 6H, N(CH₃)₂), 4.08 (s, 2H, NH₂), 6.68 (d, *J* = 8.4 Hz, 4H, ArH), 7.33 (d, *J* = 15.3 Hz, 1H, COC=CH), 7.52 (d, *J* = 8.7 Hz, 2H, ArH), 7.74 (d, *J* = 15.3, 1H, COCH=C), 7.91 (d, *J* = 8.4, 2H, ArH). ¹³C NMR (CDCl₃, 75 MHz,

ppm) δ: 40.13 (C of N(CH₃)₂), 111.80, 113.87, 116.80, 123.04, 129.25, 130.07, 130.73, 144.06, 150.58, 151.70 (C of Aromatic rings and attached alkene part), 188.34 (C=O). Elemental analysis (Perkin–Elmer 240B elemental analyzer) Calculated for: C₁₇H₁₈N₂O (%) Calculated C = 76.69, H = 6.76, N = 10.54, O = 6.01; Found C = 76.10, H = 7.00, N = 9.98, O = 5.90.

X-Ray Diffraction Crystallography

Data were collected from selected crystals mounted on glass fibers. The X-ray diffraction intensity data were measured at 293 K by the X-ray scan technique on an Oxford Diffraction Xcalibur four-circle diffractometer with Eos CCD-detector using graphite mono-chromatized Mo–Kα radiation (λ = 0.71073 Å). The data were corrected for Lorentz-polarization as well as for absorption effects [33]. The structures of the compounds were solved by direct method using the program SHELXS-97, and were refined by full-matrix least-squares technique on F2 by SHELXL97 [34] Scattering factors incorporated in SHELXL97 were used. All hydrogen atoms were refined isotropically and remaining all non-hydrogen atoms were refined anisotropically in both compounds. The H atoms bonded to N atoms in compounds were located in a difference Fourier map and refined isotropically (N–H = 0.860 Å with U_{iso}(H) = 1.2 U_{eq}(N)). All other H atoms attached to carbon atoms were positioned geometrically and refined as riding atoms, with C–H = 0.930 Å (CH), with C–H = 0.960 Å (CH₃), and U_{iso}(H) = 1.2, 1.5 U_{eq}(C). The programs ORTEP-3 for Windows [35] and Mercury [36] was used in the preparation of the figures. A summary of the crystal data and other details concerning data collection and structure refinement are given in Table 1, Selected bond lengths and bond angles are in listed in Table 2, Hydrogen bonding interactions are summarized in Table 3.

Quantum Chemical Calculations

We have performed quantum chemical calculations to get insight into the molecular orbitals involve in the absorption and emission spectra. The Density Functional Theory (DFT) based methods are most suitable for the calculations for molecules of our interest. All the calculations were performed using B3LYP density functional theory method, a hybrid version of DFT and Hartree–Fock (HF) methods, in which the exchange energy from Becke's exchange functional is combined with the exact energy from Hartree–Fock theory. Along with the component exchange and correlation functionals, Becke's three parameters define the hybrid functional, specifying the extent of the exact exchange mixed in. Although these three semi-empirical

Table 1 Crystal data, data collection and structure refinement for the compounds **1** and **2**

Compound	1	2
Crystal data		
CCDC	823222	864877
Molecular formula	C ₁₃ H ₁₇ NO ₃	C ₁₇ H ₁₈ N ₂ O
Molecular weight	235.28	266.33
Crystal system	Orthorhombic	Orthorhombic
Space group	<i>Pbca</i>	<i>P2₁2₁2₁</i>
Temperature (K)	293	293
<i>a</i> (Å)	11.7220 (12)	6.1146 (5)
<i>b</i> (Å)	14.4580 (13)	9.0567 (8)
<i>c</i> (Å)	15.7853 (12)	26.079 (3)
<i>V</i> (Å ³)	2675.2 (4)	1444.2 (2)
α (°)	90	90
β (°)	90	90
γ (°)	90	90
<i>Z</i>	8	4
<i>D</i> (Mg m ⁻³)	1.168	1.225
<i>F</i> (000)	1134	642
μ (mm ⁻¹)	0.08	0.08
Radiation λ (Å)	Mo Ka (0.71073)	Mo Ka (0.71073)
Crystal dimensions (mm)	0.36 × 0.35 × 0.34	0.37 × 0.36 × 0.35
Data collection		
<i>T</i> _{min} / <i>T</i> _{max}	0.967/1.000	0.857/1.000
θ _{max} (°)	29.2	29.0
θ _{min} (°)	3.4	3.1
<i>h</i>	−15 → 8	−6 → 8
<i>k</i>	−17 → 18	−11 → 12
<i>l</i>	−21 → 18	−34 → 32
Measured reflections	7,360	5,487
Independent reflections	2,871	3,150
Reflections with <i>I</i> > 2σ(<i>I</i>)	1,621	2,225
<i>R</i> _{int}	0.037	0.024
Refinement		
Refinement on	<i>F</i> ²	<i>F</i> ²
<i>R</i> [<i>F</i> ² > 2σ(<i>F</i> ²)]	0.045	0.050
<i>wR</i> (<i>F</i> ²)	0.091	0.079
<i>S</i>	0.96	0.99
Number of reflections	2,871	3,150
Number of parameters	154	181
Weighting scheme, <i>w</i> , <i>P</i> = (<i>F</i> _o ² + 2 <i>F</i> _c ²)/3	1/[σ ² (<i>F</i> _o ²) + (0.0308 <i>P</i>) ²]	1/[σ ² (<i>F</i> _o ²) + (0.0227 <i>P</i>) ²]
(Δ/σ) _{max}	0.011	< 0.001
Δρ _{min} , Δρ _{max} (eÅ ⁻³)	−0.09, 0.11	−0.10, 0.11

parameters are optimized aiming primarily to reproduce thermo-chemistry of small organic molecules, it has been shown to perform exceptionally well for relatively larger organic molecules of heteroatom. The geometry of the compounds were optimized at the B3LYP/6-31G(d,p) level of theory. TD-DFT calculations were performed in

conjunction with the Polarizable Continuum Model (PCM) for salvation (the energy in solution by making the solvent reaction field self-consistent with the solute electrostatic potential) in methanol to obtain absorption band, theoretically. All the calculations were carried out using Gaussian 09 suits of program [37].

Table 2 Experimental and theoretical results of selected molecular structure parameters

Compound 1		
	Experimental	B3LYP/6-31G (d,p)
Bond lengths (Å)		
O3–C9	1.3364 (16)	1.353
O3–C10	1.4731 (16)	1.476
O2–C9	1.2015 (15)	1.217
N–C9	1.3598 (18)	1.381
N–C6	1.3910 (16)	1.401
O1–C2	1.2133 (16)	1.223
C3–C2	1.4776 (18)	1.493
C2–C1	1.487 (2)	1.521
Bond angles (°)		
C9–O3–C10	121.81 (12)	121.0
C9–N–C6	128.18 (11)	128.7
C9–N–H0	115.9	114.5
C6–N–H0	115.9	116.8
O2–C9–O3	126.28 (13)	126.6
O2–C9–N	125.99 (12)	125.7
O3–C9–N	107.72 (12)	107.6
O1–C2–C3	120.07 (13)	120.9
O1–C2–C1	120.34 (14)	120.3
C3–C2–C1	119.58 (14)	118.8
O3–C10–C13	110.58 (12)	109.8
O3–C10–C11	101.98 (12)	102.4
O3–C10–C12	109.19 (12)	109.9
Compound 2		
	Experimental	B3LYP/6-31G (d,p)
Bond lengths (Å)		
C10–C9	1.437 (2)	1.453
C8–C9	1.327 (2)	1.351
C1–C8	1.473 (2)	1.479
C1–C2	1.468 (2)	1.495
O1–C1	1.2357 (18)	1.234
C5–N1	1.363 (2)	1.388
N2–C13	1.372 (2)	1.380
N2–C17	1.439 (2)	1.452
N2–C16	1.444 (2)	1.452
Bond angles (°)		
C13–N2–C17	121.86 (16)	120.2
C13–N2–C16	120.69 (15)	120.0
C17–N2–C16	117.44 (16)	119.7
C5–N1–H1A	120.0	116.1
C5–N1–H1B	120.0	116.1
H1A–N1–H1B	120.0	112.8
O1–C1–C2	120.30 (15)	119.7
O1–C1–C8	119.37 (16)	120.9
C2–C1–C8	120.33 (16)	119.3

Table 2 continued

Compound 2		
	Experimental	B3LYP/6-31G (d,p)
C9–C8–C1	120.69 (16)	120.1
C9–C8–H8	119.7	120.8
C1–C8–H8	119.7	119.1
C8–C9–C10	130.91 (18)	128.5
C8–C9–H9	114.5	115.4
C10–C9–H9	114.5	116.1

Table 3 Hydrogen bond geometry of compounds 1 and 2 (Å, °)

D–H...A	d(D–H)	d(H...A)	d(D...A)	<(DHA)
1				
N–H0...O1 ⁱ	0.86	2.081(1)	2.909(1)	161.42(8)
C7–H7...O2 ^{iv}	0.93	2.360(1)	2.934(2)	119.67(9)
C12–H12C...O2 ^{iv}	0.96	2.467(1)	3.050(2)	119.0(1)
C13–H13A...O2 ^{iv}	0.96	2.452(1)	3.010(2)	116.9(1)
2				
N1–H1B...O1 ⁱⁱ	0.86	2.125(1)	2.968(2)	166.2(1)
C6–H6...N2 ⁱⁱⁱ	0.93	2.749(2)	3.399(2)	127.6(1)
C9–H9...O1 ^{iv}	0.93	2.382(1)	2.758(2)	104.0(1)

Symmetry operations: (i) $x, -1/2 - y, -1/2 + z$ (ii) $2 - x, -1/2 + y, 1/2 - z$ (iii) $-1/2 + x, 1.5 - y, -z$ (iv) x, y, z

Results and Discussion

Hydrogen Bonding Patterns and Crystal Structure

Etter introduced graph-set notation for the characterization and analysis of hydrogen-bond patterns [38, 39]. The most remarkable feature of the graph set approach is to analyze the hydrogen-bond patterns in the complicated networks that can be reduced to combinations of simple patterns [38–40]. Mercury [36] was also used for the analysis of these patterns in both compounds behalf on X-ray analysis of crystals. The (4-acetylphenyl)amino 2,2-dimethylpropanoate (**1**) crystallized in an orthorhombic system with one molecule in asymmetric unit with Pbc_a space group and having unit cell parameters $a = 11.7220(12)$ Å, $b = 14.4580(13)$ Å, $c = 15.7853(12)$ Å, $\beta = 90^\circ$, $V = 2675.2$ (4) Å³, $Z = 8$. The molecule has one hydrogen that is participating in an intermolecular hydrogen bonding (**a**). The most likely acceptor for that hydrogen is the oxygen (**O1**) of carbonyl group, although carbonyl oxygen (**O2**) of *tert*-butyl ester group is participating in three (*b*, *c* and *d*) weak intramolecular hydrogen bonding with neighbouring hydrogens. The intermolecular hydrogen bonding

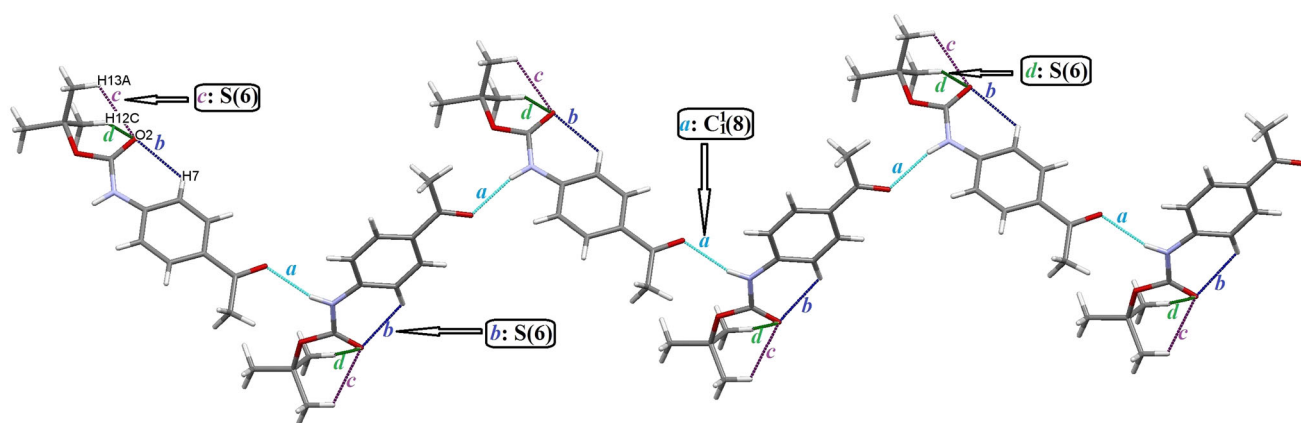


Fig. 1 Patterns in hydrogen bonding for (4-acetylphenyl)amino 2,2-dimethylpropanoate (**1**), the structure of the compound **1** forming the $C_1(8)$ chain pattern typical of many $N-H\cdots O=C$ hydrogen bond. This

difunctionality of the molecule leads to a chain structure and three different intramolecular $C-H\cdots O=C$ hydrogen bonds lead to same $S(6)$ motifs

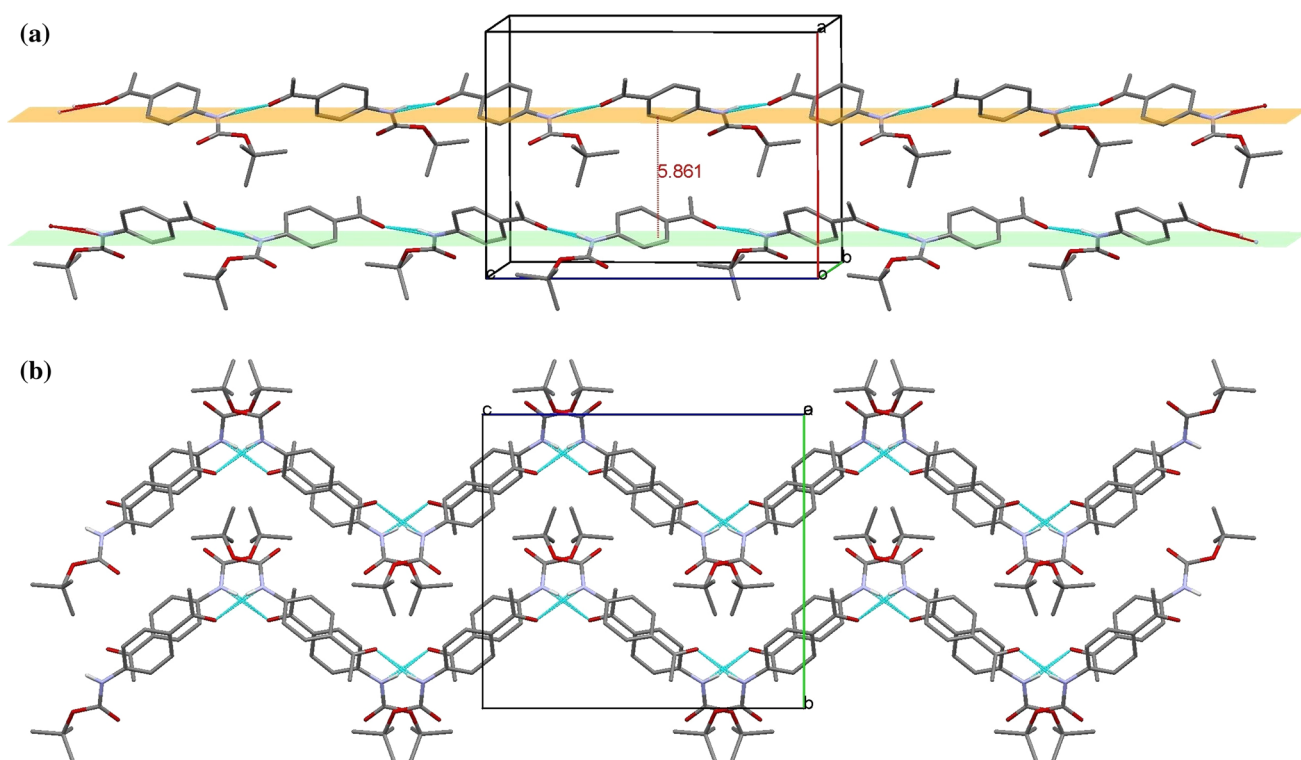


Fig. 2 In compounds **1**. **a** The distance between two antiparallel chains in a unit cell is 5.861 Å (other two chains and non significant hydrogen atoms are omitted for reasons of clarity); **b** Packing diagram showing the zig-zag arrangement along a axis by flipping 90°

(a) between $N-H\cdots O=C$ hydrogen bond is forming a chain $C_1(8)$ motif (Fig. 1). The hydrogen atoms (H13A, H12C) on tert-butyl group formed an intramolecular hydrogen bonding with O2 which is not crystallographically equivalent and we denoted it as different hydrogen bonds (c , d). The aromatic hydrogen (H7) formed hydrogen bond between $C7-H7\cdots O2$ with same carbonyl oxygen (O2) is denoted as b . The three types of intramolecular

hydrogen bonds ($C13-H13A\cdots O2$, $C12-H12C\cdots O2$, $C7-H7\cdots O2$) exhibited $S(6)$ motifs (Fig. 1). Thus first-level unitary graph set is $N_1: C_1(8)S(6)S(6)S(6)$ for compound **1**. In crystal packing of compound **1**, four molecular chains are in unit cell and arranged in two pair of layers along perpendicular to a screen by flipping 90° around a axis as shown in Fig. 2b. Each chain of each pair of layers are arranged in antiparallel manner i.e., in one chain the

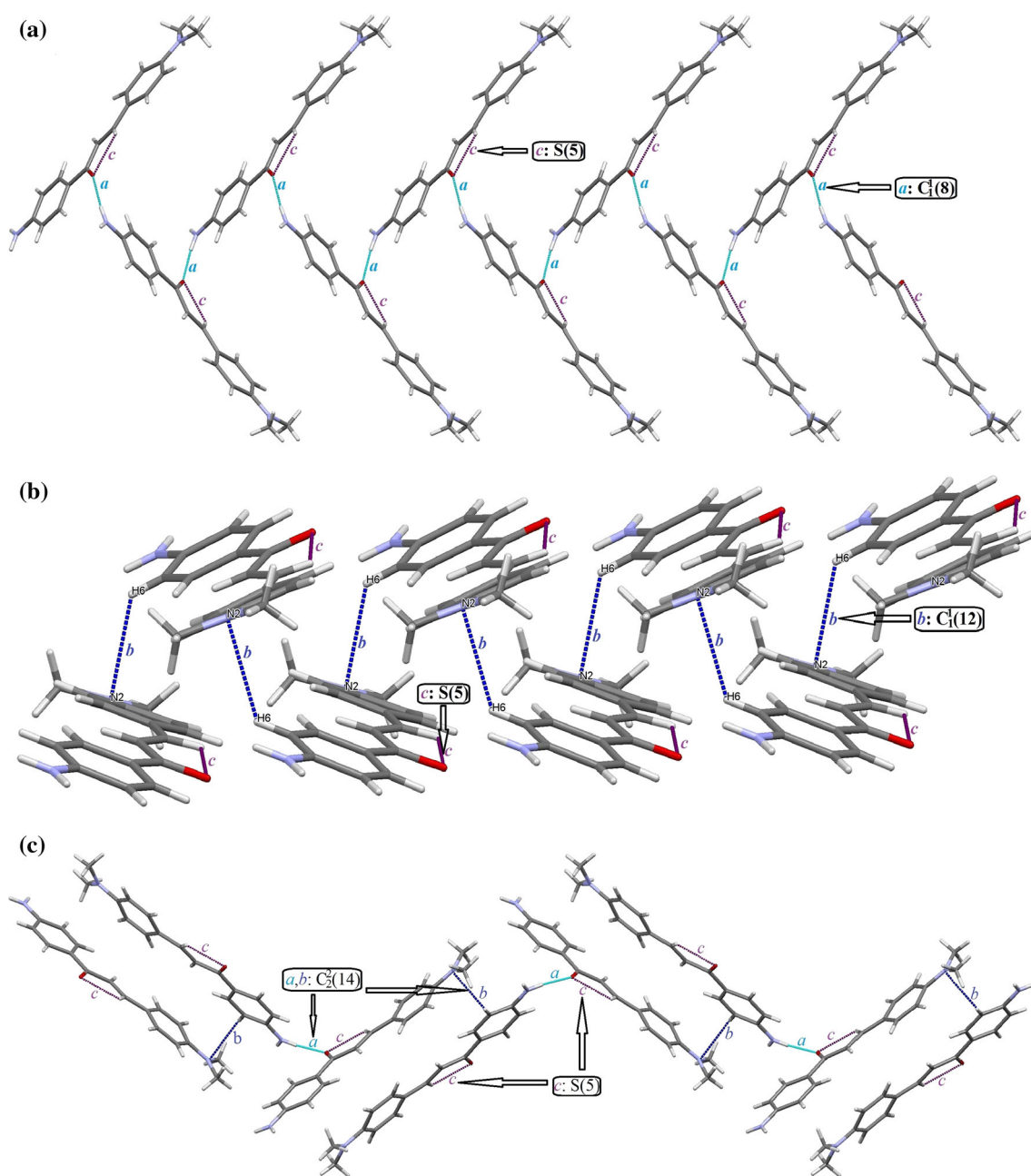


Fig. 3 Patterns in hydrogen bonding for (E)-1-(4-aminophenyl)-3-[4-(dimethylamino)phenyl]prop-2-en-1-one (**2**), forming the $C_1^1(8)$ and $C_1^1(12)$ chain pattern connecting through N–H...O=C (a) and N...H–C

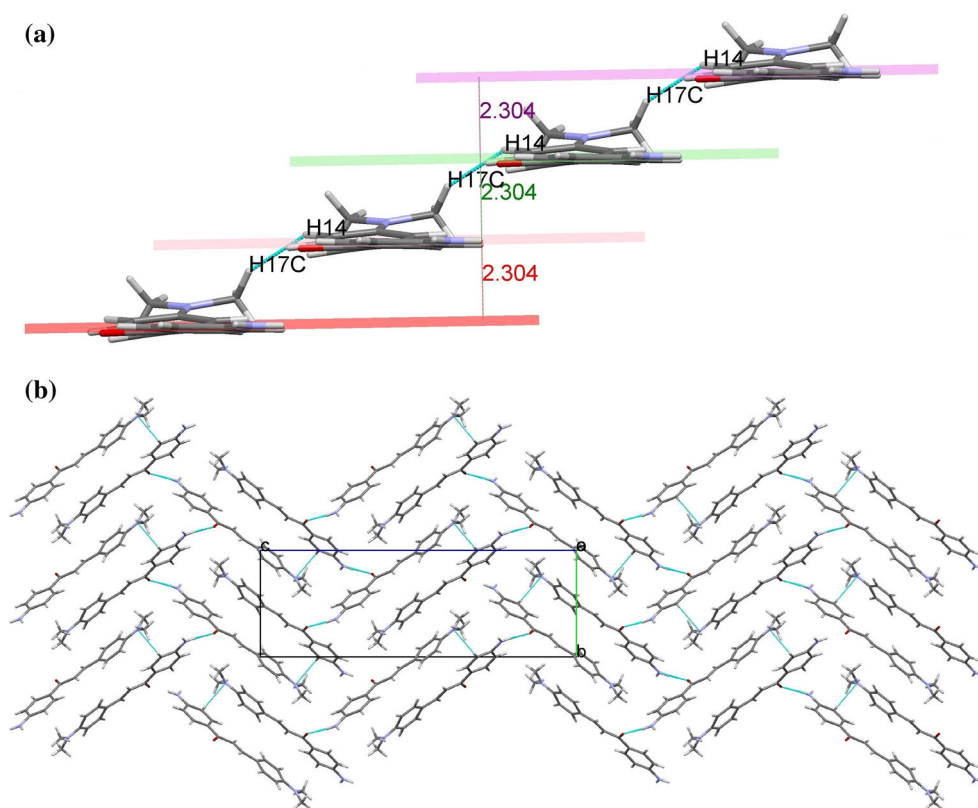
(b) hydrogen bonds respectively and one intramolecular motif $S(5)$ connected C–H...O=C (c) hydrogen bond

molecules are arranged head to tail while in other chain molecules are tail to head arrangement, and distance between planes of each chain is 5.861 Å as shown in Fig. 2a. Molecules of each chain are connected with strong N–H...O (*a*) classical intermolecular hydrogen bonding (Fig. 1), these strong H-bonding is stabilizing crystal packing. The arrangements of molecules in crystal packing looks like a zig-zag fashion as seen in Fig. 2b. The

distance between donor hydrogen and acceptor atom (H...A) in strong intermolecular hydrogen bonding (H0...O1) is 2.08 Å while in weak intramolecular Hydrogen bonding H7...O2, H12C...O2, H13A...O2 are 2.36, 2.47, 2.45 Å. (Table 3).

In compound (E)-1-(4-aminophenyl)-3-[4-(dimethylamino)phenyl]prop-2-en-1-one (**2**), one molecule is present in asymmetric unit and it crystallizes in orthorhombic system with

Fig. 4 In compound **2**. **a** The non-classical (C14–H14...H17–C17) interactions were forming the stepwise layer and height of each step is 2.304 Å in each layer; **b** Packing diagram showing the zig-zag arrangement along a axis by flipping 90°



unit cell parameters, $a = 6.1146(5)$ Å, $b = 9.0567(8)$ Å, $c = 26.079(3)$ Å, $\beta = 90^\circ$, $V = 1444.2(2)$ Å³, $Z = 4$ in $P2_12_12_1$ space group. The molecule forms a $C_1^1(8)$ motif by an intermolecular $N\cdots H\cdots O=C$ (*a*) hydrogen bond between an amino hydrogen (H1B) and carbonyl oxygen (O1) (Fig. 3a) and on the other hand, *N,N*-dimethyl amino groups with aromatic hydrogen (H6) form $N\cdots H\cdots C$ (*b*) hydrogen bond, leading to the $C_1^1(12)$ motif (Fig. 3b). The hydrogen atom (H9) on $C=C$ double bond leads to $S(5)$ motif for each molecule. These motifs are unitary level, hence the first-level graph set is $N_1: C_1^1(8)C_1^1(12)S(5)$. Second-level graph set (binary graph set) was also present in same molecule, as we have discussed above, the motifs $C_1^1(8)$ and $C_1^1(12)$ for the two hydrogen bonds *a* and *b*, give the unitary graph set $C_1^1(8)C_1^1(12)$ leaving the intramolecular hydrogen bond $S(5)$ motif. These two hydrogen bonds (*a*, *b*) form a chain $C_2^2(14)$, represents a binary graph set $N_2(a,b): C_2^2(14)$ (Fig. 3c). Crystal structure of compound **2** is more complicated in comparison to compound **1**. The non-classical (C14–H14...H17–C17) interaction is found forming the stepwise layer with height of each step equal to 2.304 Å (mean plane of both benzene ring of chalcone is considered as floor of step) in crystal packing shown in Fig. 4a. The packing of molecules look like in a zig-zag manner by flipping 90° around a axis shown in Fig. 4b. The distance of strong intermolecular hydrogen bonding between H1B...O1 is 2.13 Å while the distance between O1...H9, N2...H6, H17C...H14 interactions are 2.38, 2.75, 2.31 Å respectively.

Structural Analysis

The solid state structure of compounds **1** and **2** was determined by X-ray analysis and their optimized geometries, presented in Fig. 5. The geometric parameters of **1** and **2** were calculated at the B3LYP/6-31G(d,p) level by DFT method and listed in Table 2, along with corresponding experimental values. As seen in Table 2, most of the predicted geometric parameters have minute higher values than those determined experimentally. This shows a good agreement with experimental. Comparing the predicted values with the experimental ones, it was found that the largest difference in bond lengths occurs between C2–C1 (same nomination in both) bond with a difference of 0.034 and 0.027 Å in both compounds **1** and **2**, respectively. Considering the bond angles, the highest variation seems in between the experimental and predicted values can be found at bond angle C9–N–H0 for **1** and C5–N1–(H1A/H1B) for **2** with the difference of 1.40° and 3.90°, respectively. This is due to the fact that the experimental data described for compound **1** and **2** in the solid state, whereas the calculated data correspond to the molecule in the gaseous phase. The geometry of the solid-state structure is subject to intermolecular forces, such as van der Waals interactions, crystal packing forces, hydrogen-bond interactions. For example, $N\cdots H\cdots O$, $C\cdots H\cdots N$ and $C\cdots H\cdots O$ H-bonds as described in hydrogen bonding patterns in both

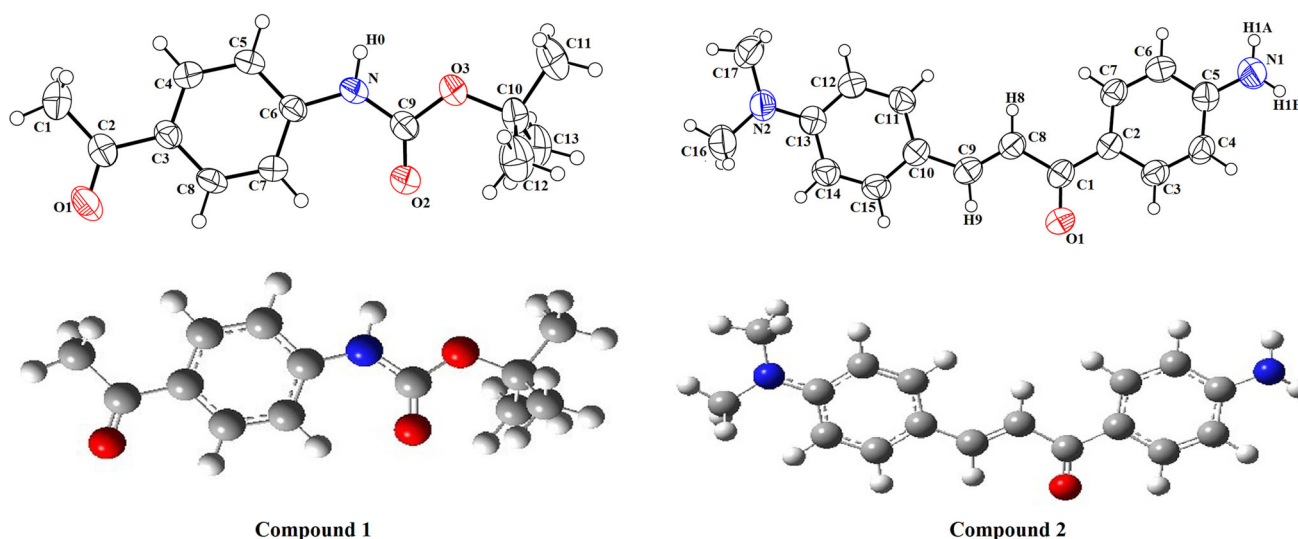


Fig. 5 Molecular view of compounds; X-ray structure (*above*) and optimized structure (*below*)

compounds, which make the experimental geometric parameters differences from the calculated ones and other region of being difference in angles may be due to resonance of nitrogen lone pair in aromatic rings, giving trigonal planer in X-ray structure.

Vibrational Analysis

The vibrational frequencies of compound **1** and **2** were calculated at the B3LYP/6-31G(d,p) level of theory and IR spectra were plotted using Molden viewing package. These spectra are shown in Fig. 6 along with the corresponding experimental spectra for comparison. The major experimental and calculated frequencies are also summarized in Table 4. There were deviations in infrared intensities between the experimental data and the calculated data, some peaks could not be found in the experiment data but they are present in the calculated data. Comparison of the calculated frequencies with the experimental values reveals overestimation of the predicted vibrational modes. Any discrepancy noted between the observed and calculated frequencies may be due to the two facts: one is that the experimental results belong to solid phase whereas theoretical calculations were performed in gaseous phase; the other is that the calculations were actually done on a single molecule while the experimental values recorded in the presence of intermolecular interactions. Peaks found in the calculated and the experimental spectra are important and are as per presence of functional groups in both compounds. The strongest peak in calculated spectra by the DFT method in compound **1** appeared at 1,808 and 1,772 cm^{-1} , while in

the experimental spectrum strongest peaks appeared at 1,722 and 1,666 cm^{-1} respectively which are representing the two C=O stretching bond. In compound **2**, C=O stretching frequency appeared 1,728 cm^{-1} in calculated spectra by DFT method while in experimental spectra it appeared at 1,644 cm^{-1} . The lowering of experimental values are well understood due to strong N–H...O=C hydrogen bonding as well as conjugation in both compounds. The N–H bond stretching vibration observed at 3,253 cm^{-1} experimentally whereas in calculated spectra it appeared at 3,634 cm^{-1} in compound **1**. In compound **2**, amino group $\nu_{\text{N-H}}$ appeared at 2,895 cm^{-1} (asymmetric), 2,854 cm^{-1} (symmetric) while predicted theoretically at 3,691, 3,581 cm^{-1} . The predicted bands of the –NH in-plane bending for compound **1** and **2**, which were located at 1,563 and 1,656 cm^{-1} (B3LYP/6-31G(d,p) level), were evident in the IR spectrum at 1,587 and 1,568 cm^{-1} . The results, obtained by the B3LYP/6-31G(d,p) method, were in agreement with those of the experiment in finger print region but deviation in functional group region. The large deviation in vibrational frequencies may be because of level of theory adopted i.e., B3LYP/6-31G(d,p) and one has to introduce scaling factors to reduce deviations [41] while comparing theoretically predicated IR frequencies with that of experimentally observed data.

Frontier Molecular Orbitals and Electronic Spectra

The frontier molecular orbitals play an important role in the electric and optical properties, as well as in UV–vis spectra and chemical reactions [42]. The basic electronic parameters related to the frontier orbitals in a molecule are

Fig. 6 Infrared spectrum of the compounds; experimental (*above*) and theoretical (*below*)

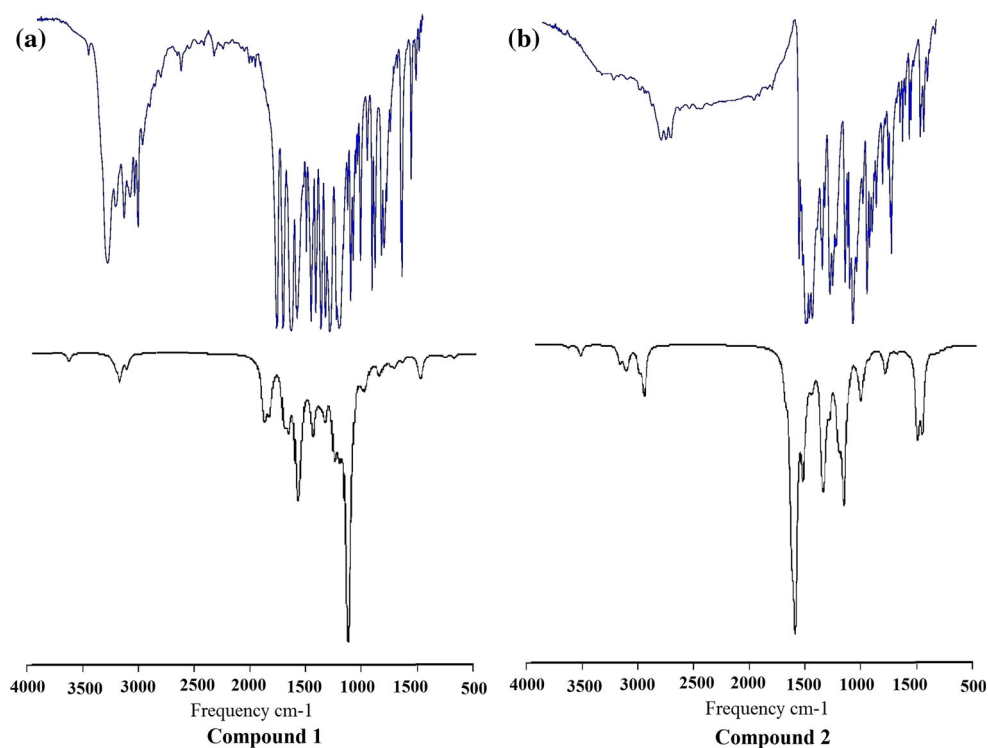


Table 4 Assignments of experimental and calculated vibrational frequencies (cm^{-1})

Compound 1			Compound 2		
Vibrational assignments ^a	Experimental ^b	B3LYP/6-31G(d,p)	Vibrational assignments ^a	Experimental ^b	B3LYP/6-31G(d,p)
$\nu_{\text{N-H}}$	3,253s	3,634	$\nu_{\text{N-H}}^{\text{as}}$	2,895m	3,691
$\nu_{\text{C-H}}$	3,183ms	3,173	$\nu_{\text{N-H}}^{\text{s}}$	2,854m	3,581
$\nu_{\text{C-H}}^{\text{as}}$	3,104ms	3,110	$\nu_{\text{C-H}}$	2,806m	3,217
$\nu_{\text{C-H}}^{\text{as}}$	3,049ms	3,053	$\nu_{\text{C=O}}$	1,644s	1,728
$\nu_{\text{C-H}}^{\text{s}}$	3,008ms	3,061	$\delta_{\text{N-H}}$	1,568vs	1,656
$\nu_{\text{C-H}}^{\text{s}}$	2,976ms	3,047	$\nu_{\text{C=C}}$	1,551vs	1,616
$\nu_{\text{C=O}}$	1,722vs	1,808	$\nu_{\text{C=C}}$	1,525vs	1,572
$\nu_{\text{C=O}}$	1,666vs	1,772	$\delta_{\text{C-H}}$	1,433s	–
$\delta_{\text{N-H}}$	1,587vs	1,563	$\nu_{\text{C-N}}$	1,364s	1,400
$\nu_{\text{C=C}}$	1,537s	1,661	$\nu_{\text{C-N}}$	1,339s	1,378
$\nu_{\text{C=C}}$	1,455ms	1,453			
$\delta_{\text{C-H}}$	1,411s	1,413			
$\delta_{\text{C-H}}$	1,370s	1,393			
$\delta_{\text{C-H}}$	1,321s	1,338			
$\nu_{\text{C-N}}$	1,281s	1,254			

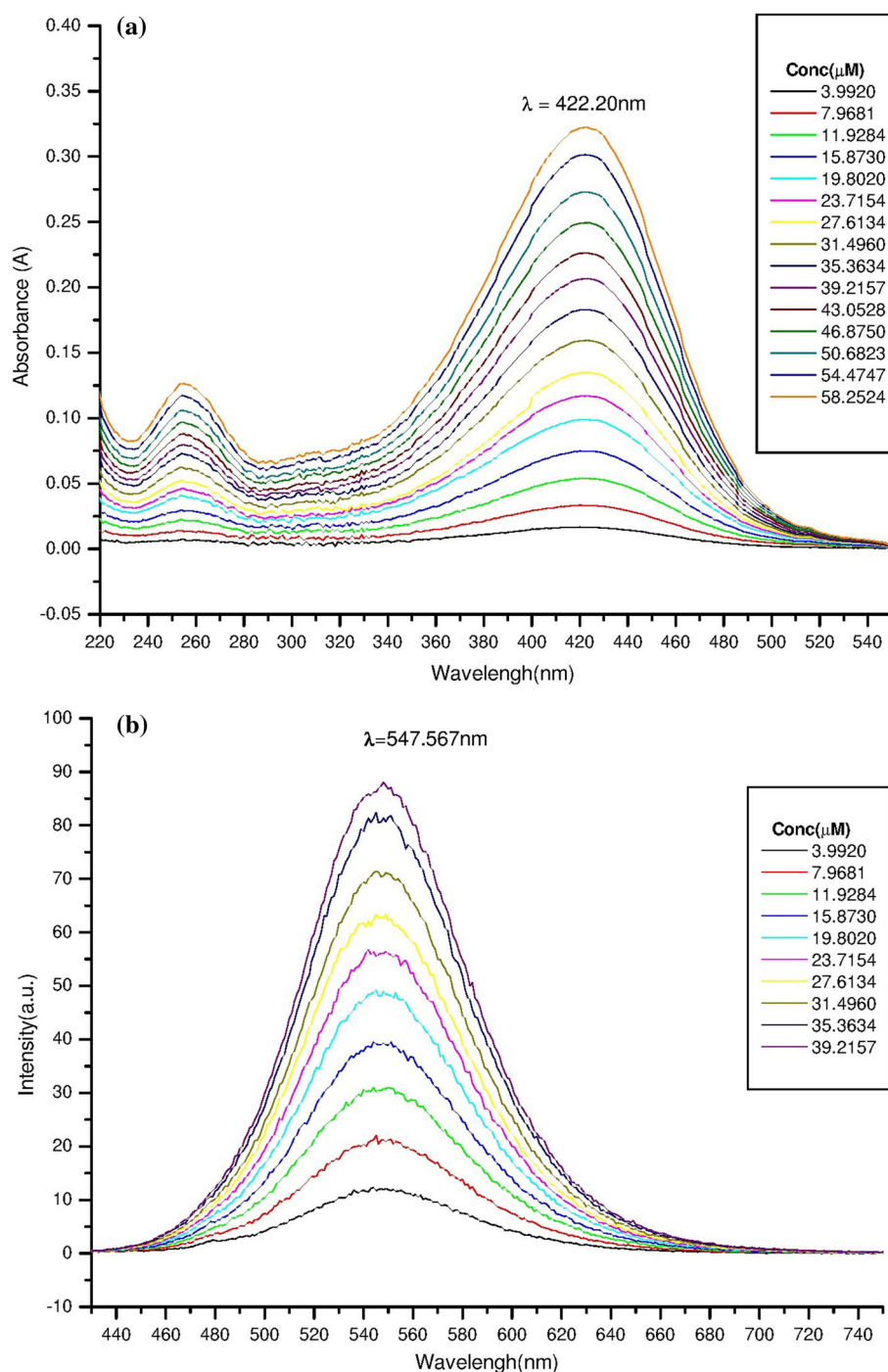
^a ν stretching, δ bending in plan, *as* asymmetric, *s* symmetric

^b *s* strong, *ms* medium strong, *vs* very strong, *m* medium

the highest occupied molecular orbital (HOMO) and lowest unoccupied molecular orbital (LUMO) and their resulting energy gaps. These orbitals not only determine the way the molecule interacting with other species but their energy gaps (frontier orbital gaps) help in characterizing the

chemical reactivity of the molecule. The frontier molecular orbitals and their energy levels are computed at B3LYP/6-31G(d,p) level. As evidence of this theory for electronic spectra, electronic absorption spectra was calculated with TD-DFT method, based on the B3LYP/6-31G(d,p) level

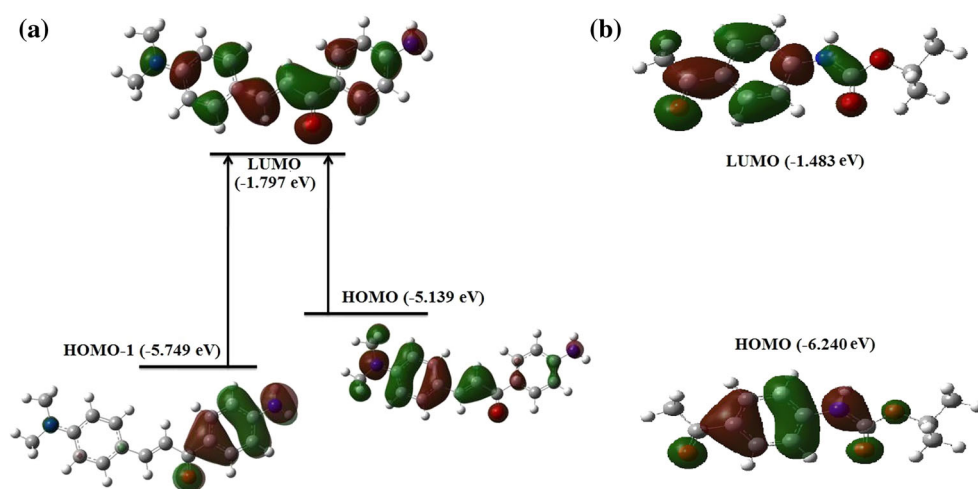
Fig. 7 Absorption (a) and fluorescence (b) spectra of (E)-1-(4-aminophenyl)-3-[4-(dimethylamino)phenyl]prop-2-en-1-one



optimized structure of the compounds. Figure 7a shows the UV–vis spectra of (E)-1-(4-aminophenyl)-3-[4-(dimethylamino)phenyl]prop-2-en-1-one (**2**) in methanol solvent at various concentrations. It is evident that there is no significant change in shape of absorption spectra, is due to that as concentration increases there is no molecular aggregation in methanol solvent. The compound **2** displays a main absorption band centered at 422.20 nm. A TD-DFT calculation indicates that the lowest energy transition at

407.08 nm can be correlated to the experimentally observed band. This transition mainly composed of HOMO to LUMO and HOMO-1 to LUMO excitations. From the frontier MO pictures (depicted in Fig. 8a) it is discernible that the electronic excitations take place from both the aromatic ring of the molecule. The second absorption peak near 260.00 nm can mostly be attributed to transitions from HOMO-5, HOMO-4, HOMO-3 to LUMO. Our inspection of frontier MOs indicates that these transitions also involve

Fig. 8 **a** Frontier molecular orbitals (FMOs) involved in the absorption of **2**, and **b** HOMO–LUMO of **1**



excitations of aromatic ring electrons. The room temperature emission spectra of **2** is presented in Fig. 7b. When the compound **2** is excited at 422.20 nm, it fluoresces at 547.56 nm. The influence of concentration in methanol solvent on fluorescent behavior was also investigated as shown in Fig. 7b. The latter compound (4-acetylphenyl)amino 2,2-dimethylpropanoate (**1**) was not showed UV–vis and photoluminescence spectra experimentally. Our TD-DFT calculation indicates that compound **1** does not absorbed in the range of wavelength considered in the present study.

Mulliken Atomic Charges

Mulliken charge distributions were calculated from the Mulliken population analysis at the B3LYP/6-31G(d,p) level. The computed Mulliken charge values on each atom of compounds **1** and **2** are listed in Table 5. The carbon atoms attached with any electronegative atom exhibited positive charges in both compounds. Carbon atom C3 of compound **1** and carbon atoms C2, C7, C10 of compound **2** are not attached to any electronegative atom, but show positive charge. The all electronegative atoms N(−0.657), O1(−0.461), O2(−0.509) and O3(−0.536) in compound **1** exhibited negative charge in the range −0.657 to −0.461 a.u., while in compound **2**, N1(−0.657), N2(−0.509) and O1(−0.520) atoms exhibited negative charge in the range −0.657 to −0.509 a.u. The methyl carbon atoms, C1 of compound **1** and C16 (C17) of compound **2** are most negative carbon atoms and having charges −0.399, −0.169 (−168) a.u., respectively. One should however, note that these atoms cannot act as donor site. On the other hand, most negative atom is N of compound **1** and N1 of compound **2**, both contains same charge −0.657 a.u. and they act as good donor site. Overall compound **1** has four donor sites (N, O1, O2, O3) while there are three (N1, N2 and O1) in compound **2**.

Conclusions

The graph set of hydrogen bonding patterns and DFT studies of (4-acetylphenyl)amino 2,2-dimethylpropanoate (**1**) and (E)-1-(4-aminophenyl)-3-[4-(dimethylamino)phenyl]prop-2-en-1-one (**2**) are reported for the first time. The formation of these compounds were also confirmed by spectroscopic analysis. Slow evaporation solution growth method was employed to grow single crystals of good quality for X-rays diffraction. Compound **1** is prepared by protection of 4-aminoacetophenone with di-*tert*-butyldi-carbonate while compound **2** (Chalcone) was prepared by Claisen-Schmidt condensation method with 4-dimethylaminobenzaldehyde. Compound **1** exhibited four different motifs, one chain $C_1^1(8)$ motif connecting through N–H...O hydrogen bond and three intramolecular hydrogen bonds (C13–H13A...O2, C12–H12C...O2, C7–H7...O2) exhibited same $S(6)$ motifs, these motifs give unitary graph set $N_1: C_1^1(8)S(6)S(6)S(6)$. The compound **2** is leading three motifs, two chains $C_1^1(8)$ and $C_1^1(12)$ connected N–H...O, and N...H–C hydrogen bonds respectively and one $S(6)$ as a first-level graph set $N_1: C_1^1(8)C_1^1(12)S(6)$, but involving both H-bonds *a* and *b* gives binary graph set $N_2(a,b): C_2^2(14)$. The arrangement of molecules in each compound is zig-zag type with same orthorhombic crystal system. Molecular geometries and vibrational spectra of the compounds were investigated using the DFT method. The TD-DFT calculations in the solution (methanol) were used to predict the nature of the electronic transitions observed in the absorption spectra, the assignment and analysis of the electronic transitions were performed using the frontier molecular orbitals. The calculated geometry of both compounds is in good agreement with the X-ray crystallographic data and the calculated vibrational spectra compare well with the experimental data but showing some variations.

Table 5 Mulliken atomic charges of compounds (**1** and **2**)

Atoms	B3LYP/6-31G(d, p)
Compound 1	
C1	−0.399
C2	0.389
C3	0.054
C4	−0.127
C5	−0.142
C6	0.335
C7	−0.099
C8	−0.121
C9	0.822
C10	0.267
C11	−0.309
C12	−0.323
C13	−0.322
N	−0.657
O1	−0.461
O2	−0.507
O3	−0.536
Compound 2	
C1	0.371
C2	0.035
C3	−0.104
C4	−0.120
C5	0.297
C6	−0.123
C7	0.117
C8	−0.152
C9	−0.095
C10	0.130
C11	−0.125
C12	−0.136
C13	0.355
C14	−0.137
C15	−0.143
C16	−0.169
C17	−0.168
N1	−0.657
N2	−0.501
O1	−0.528

Supplementary material

CCDC-823222 for (**1**) and 864877 for (**2**) contain the supplementary crystallographic data for this paper. These data can be obtained free of charge at <http://www.ccdc.cam.ac.uk/const/retrieving.html> or from the Cambridge Crystallographic Data Centre (CCDC), 12 Union Road, Cambridge CB2 1EZ, UK; fax: + 44(0)1223-336033 or email: deposit@ccdc.cam.ac.uk.

Acknowledgments Alka Agarwal is thankful to Banaras Hindu University, Varanasi, India, for the financial assistance and are highly thankful to department of chemistry, Banaras Hindu University, Varanasi for providing FT ^1H NMR, ^{13}C NMR and single crystal X-ray diffraction facilities. Rama Kant is thankful to CSIR HRDG New Delhi, India for providing Junior Research Fellowship.

References

- Go ML, Wu X, Liu XL (2005) *Curr Med Chem* 12:483–499
- Dimmock JR, Elias DW, Beazely MA, Kandepu NM (1999) *Curr Med Chem* 6:1125–1149
- Xia Y, Yang ZY, Xia P, Bastow KF, Nakanishi Y, Lee KH (2000) *Bioorg Med Chem Lett* 10:699–701
- Bois F, Beney C, Boumendjel A, Mariotte AM, Conseil G, Di Pietro A (1998) *J Med Chem* 41:4161–4164
- Liu M, Wilairat P, Go ML (2001) *J Med Chem* 44:4443–4452
- Hsieh HK, Lee TH, Wang JP, Wang JJ, Lin CN (1998) *Pharm Res* 15:39–46
- Lin YM, Zhou YS, Flavin MT, Zhou LM, Nie WG, Chen FC (2002) *Bioorg Med Chem* 10:2795–2802
- Rojas J, Paya M, Dominguez JN, Ferrandiz ML (2002) *Bioorg Med Chem Lett* 12:1951–1954
- Ducki S, Forrest R, Hadfield JA, Kendall A, Lawrence NJ, McGown AT, Rennison D (1998) *Bioorg Med Chem Lett* 8:1051–1056
- Maria K, Dimitra HL, Maria G (2008) *Med Chem* 4:586–596
- Cheng JH, Hung CF, Yang SC, Wang JP, Won SJ, Lin CN (2008) *Bioorg Med Chem* 16:7270–7276
- Cheenpracha S, Karalai C, Ponglimanont C, Subhadhirasakul S, Tewtrakul S (2006) *Bioorg Med Chem* 14:1710–1714
- Svetaz L, Tapia A, Lopez SN, Furlan RLE, Petenatti E, Pioli R, Schmeda-Hirschmann G, Zacchino SA (2004) *J Agric Food Chem* 52:3297–3300
- Saavedra MJ, Borges A, Dias C, Aires A, Bennett RN, Rosa ES, Simoes M (2010) *Med Chem* 6:174–183
- Batovska DI, Todorova IT (2010) *Curr Clin Pharmacol* 5:1–29
- Torigoe T, Arisawa M, Itoh S, Fujiu M, Maruyama HB (1983) *Biochem Biophys Res Commun* 112:833–842
- Manske RH (1942) *Chem Rev* 30:113–144
- Chopde HN, Meshram JS, Pagadala R, Jetti V (2010) *Der Pharma Chemica* 2:294–300
- Mohamed MS, Kamel MM, Kassem EMM, Abotaleb N, Nofal SM, Ahmed MF (2009) *Acta Poloniae Pharmaceutica-Drug Res* 66:487–500
- Mishra V, Pandeya SN, DeClercq E, Pannecouque C, Witvrouw M (1998) *Pharm Acta Helv* 73:215–218
- Vardanyan R, Hruby V (2006) *Synthesis of essential drugs*, 1st edn. Elsevier, Amsterdam, pp 344–345
- Singh MK, Tilak R, Nath G, Awasthi SK, Agarwal A (2013) Design, synthesis and antimicrobial activity of novel benzothiazole analogs. *Eur J Med Chem*. doi:10.1016/j.ejmech.2013.02.027
- Dixit SK, Mishra N, Sharma M, Singh S, Agarwal A, Awasthi SK, Bhasin VK (2012) *Eur J Med Chem* 51:52–59
- Singh S, Singh MK, Agarwal A, Hussain F, Awasthi SK (2011) *Acta Cryst E67*:o1616–o1617
- Singh MK, Agarwal A, Awasthi SK (2011) *Acta Cryst E67*:o1137
- Singh MK, Agarwal A, Mahawar C, Awasthi SK (2011) *Acta Cryst E67*:o1382
- Agarwal A, Singh MK, Singh S, Bhattacharya S, Awasthi SK (2011) *Acta Cryst E67*:o2637–o2638
- Singh S, Singh MK, Agarwal A, Awasthi SK (2011) *Acta Cryst E67*:o3163
- Agarwal A, Singh MK, Awasthi SK (2011) *Acta Cryst E67*:o3213–o3214

30. Mahawar C, Singh MK, Agarwal A (2013) *Proc Natl Acad Sci Sect A Phys Sci* 83(3):207–212
31. Khlebnikov V, Patel K, Zhou X, Reddy MM, Su Z, Chiacchia FS, Hansen HC (2009) *Tetrahedron* 65:6932–6940
32. Mishra N, Arora P, Kumar B, Mishra LC, Bhattacharya A, Awasthi SK, Bhasin VK (2008) *Eur J Med Chem* 43:1530–1535
33. Diffraction Oxford (2009) *CrysAlis PRO*. Oxford diffraction Ltd, Yarnton
34. Sheldrick GM (2008) *Acta Cryst A* 64:112–122
35. Farrugia LJ (1997) *J Appl Crystallogr* 30:565
36. Macrae CF, Edgington PR, McCabe P, Pidcock E, Shields GP, Taylor R, Towler M, van de Streek J (2006) *J Appl Cryst* 39:453–457
37. Frisch MJ, Trucks GW, Schlegel HB et al (2010) *GAUSSIAN 09*, Revision C.01, Gaussian, Inc., Wallingford, CT
38. Etter MC (1990) *Acc Chem Res* 23:120–126
39. Etter MC, MacDonald JC, Bernstein J (1990) *Acta Cryst B* 46:256–262
40. Bernstein J, Davis RE, Shimoni L, Chang N (1995) *Angew Chem Int Ed Engl* 34:1555–1573
41. Rauhut G, Pulay P (1996) *J Phys Chem* 99:3093–3100
42. Fleming I (1976) *Frontier orbitals and organic chemical reactions*. Wiley, London